

MAGNETOHYDRODYNAMIC CONVECTIVE FLOW OF NANOFLUID IN DOUBLE LID-DRIVEN CAVITIES UNDER SLIP CONDITIONS

by

**Sameh E. AHMED^{a,b}, Zehba A. S. RAIZAH^a,
and Abdelraheem M. ALY^{a,b*}**

^a Department of Mathematics, Faculty of Science, King Khalid University, Abha, Saudi Arabia

^b Department of Mathematics, Faculty of Science, South Valley University, Qena, Egypt

Original scientific paper

<https://doi.org/10.2298/TSCI190811141A>

In this paper, we introduced a numerical analysis for the effect of a magnetic field on the mixed convection and heat transfer inside a two-sided lid-driven cavity with convective boundary conditions on its adjacent walls under the effects of the presence of thermal dispersion and partial slip. A single-phase model in which the water is the base fluid and a copper is nanoparticles is assumed to represent the nanofluid. The bottom and top walls of the cavity move in the horizontal direction with constant speed, while the vertical walls of the cavity are stationary. The right wall is mentioned at relatively low temperature and the top wall is thermally insulated. Convective boundary conditions are imposed to the left and bottom walls of the cavity and the thermal dispersion effects are considered. The finite volume method is used to solve the governing equations and comparisons with previously published results are performed. It is observed that the increase in the Hartmann number causes that the shear friction near the moving walls is enhanced and consequently the horizontal velocity component decreases.

Key words: mixed convection, periodic magnetic field, slip condition, nanofluid, convective boundary conditions

Introduction

Magnetohydrodynamic mixed convection flow and heat transfer enhancement using nanofluid attracted the attention of many researchers in the recent years. This is because many practical applications of these approaches in various industries. The nanofluid was discovered to avoid the problem of low thermal conductivity for convective heat transfer fluids. In 1995, Choi [1] presented the expression *nanofluid* to refer to the suspension containing a base fluid such as water, oil or ethylene glycol and nanoparticle such as copper or alumina. Since this date, very large number of studies were presented in this topic. The results in Eastman *et al.* [2] showed that when the copper nanoparticles disperse in ethylene glycol, this gives thermal conductivity for the suspension much higher than either pure ethylene glycol or ethylene glycol containing the same volume fraction of dispersed oxide nanoparticles. Mansour *et al.* [3] presented a comprehensive study for mixed convection of a water based nanofluid containing various types of nanoparticles inside a square enclosure with a heat source located in its bottom wall. The results indicated that the heat transfer rate was enhanced by increase the nanofluid solid fraction. Mansour and Ahmed [4] examined the effects of the governing

* Corresponding author, e-mail: abdelreheam.abdallah@sci.svu.edu.eg

parameters for mixed convection flow of a nanofluid inside double lid-driven enclosure. The Al_2O_3 -water suspension was used to represent the nanofluid and a nanolayer thickness was set to be equal 1 nm. Significant enhancements were obtained in the local Nusselt number by increase the solid volume fraction for all considered cases. Hayat *et al.* [5] presented a theoretical study for MHD boundary-layer flow and heat transfer of nanofluids over an inclined cylinder saturated in a porous medium with slip and radiation effects. The results showed that the increase in magnetic parameter leads to increase the temperature distributions. The differential transformation method is applied by Chen *et al.* [6] to solve the governing equations of MHD mixed convection flow of Al_2O_3 -water nanofluid in a vertical channel. The entropy generation analysis is, also, taken into account. It is found that the increase in Brinkman number results in an increase in the velocity profiles, while the increase in Hartmann number decreases the velocity distributions. The references Selimefendigil and Oztop [7], Rashidi *et al.* [8], and Hsiao [9] presented a comprehensive studies for MHD mixed convection flow and heat transfer of nanofluids inside lid-driven cavities, a vertical channel and over a stretching sheet, respectively. Sankar *et al.* [10] investigated the numerically the natural-convection from inner/outer walls in annular cavity. Mahajan *et al.* [11] studied the convection in a magnetic fluid for rigid-rigid and rigid-free boundary surfaces. Das *et al.* [12] considered the effects of magnetic field and variable conductivity of the thermal and electrical walls in a vertical channel filled with nanofluid.

Ismael *et al.* [13] discussed the MHD mixed convection and heat transfer in a lid-driven enclosure filled with nanofluid. A partial slip conditions are imposed to the horizontal walls of the cavity, while a heat source is embedded in the left wall. It is found that the increase in the heat source causes a reduction in the convective heat transfer. Rashad *et al.* [14] studied the effect of magnetic force and slip condition on the mixed convection inside a square enclosure involving a heat source/sink and filled with a nanofluid. Their results indicated that the heat transfer takes its maximum values when the heat source lies in the middle of the wall. Hayat *et al.* [15] applied the two-phase model for nanofluid to investigate the effects of slip condition and Hall current on peristaltic flow in a rotating frame. The presence of heat source/sink is, also, taken into account. The results of the problem showed that the velocity is reduced by increase the Hall parameter or Hartmann number. Alsabery *et al.* [16] applied the finite difference approaches to solve the PDE governing the natural-convection in a wavy porous enclosure containing a concentric solid and filled with nanofluid. It is found that non-uniform heating acts as a retarding force for heat transfer rate. Djoko and Koko [17] presented a numerical treatment for both Stokes and Navier Stokes equations in two and 3-D in the presence of non-linear slip conditions. Abbas and Sheikh [18] reported on the boundary-layer stagnation point flow of water and kerosene as a based ferro-fluid and manganese zinc ferrite ($\text{Mn-ZnFe}_2\text{O}_4$), cobalt ferrite (CoFe_2O_4), and magnetite (Fe_3O_4) as ferro-particles in the presence of non-linear slip conditions and homogeneous/heterogeneous reactions. Variable thermal radiation and thermal conductivity influences on MHD mixed convection flow of nanofluid along a stretching plate including slip and convective boundary conditions were examined by Akbar and Khan [19]. The results indicated that the increase in the nanoparticle volume fraction enhances the velocity and boundary-layer thickness. Mansour *et al.* [20] investigated the unsteady MHD double diffusive convection of micropolar fluid over a vertical plate saturated porouse medium with slip effect.

Murthy *et al.* [21] discussed the influences of convective boundary conditions on MHD convective flow of nanofluid along a vertical plate saturated in a non-Darcy porous medium. Aziz [22] discussed the Blasius flow along a flat plate under convective boundary conditions. Makinde and Aziz [23] studied effects of the convective boundary conditions on the mixed con-

vection of nanofluids past a stretching surface. Ishak [24] investigated the boundary-layer flow and heat transfer over a permeable surface in the presence of convective boundary conditions. The heat transfer by mixed convection boundary-layer flow at a general 3-D stagnation point using nanofluid was presented by Bachok *et al.* [25]. Ahmad and Pop [26] presented a numerical study for heat transfer and boundary-layer flow over a vertical flat plate saturated a porous medium using nanofluids. Bataller [27] applied similarity solutions to investigate the flow and heat transfer of a quiescent fluid past a non-linearly stretching plate.

In many of the previous studies, the authors considered the case of MHD and partial slip as in [13-15] but they neglected case of the variable magnetic field and effects of convective boundary conditions. In addition, the authors in references [21-27] considered the effects of the convective boundary conditions but they studied them on case of boundary-layer flow and neglected cases of internal flow and MHD. Until now, there is no any investigation was presented to discuss the MHD mixed convection and heat transfer of nanofluid inside a lid-driven cavity with partial slip under convective boundary conditions. Therefore, the objective of this paper is to collect all these neglected cases. The solid particle dispersion effects are taken into account. In this area of the research, most of the experimental correlations are defined in terms of the non-dimensional forms. In addition, most of the numerical studies solve the non-dimensional equations. Then, the finite volume method with SIMPLE algorithm is applied to solve the non-dimensional governing equations. The effects of the dimensionless quantities including Biot number, slip parameter, nanoparticle volume fraction and Hartmann number on the flow field and heat transfer characteristics are presented and discussed.

Problem description

Figure 1 shows the physical model for a steady 2-D, laminar flow of an incompressible, viscous, electrical conducting nanofluid inside an enclosure with height, H . It is assumed that, convective boundary conditions are imposed to the left and bottom walls, while the right and top walls are cold and insulated, respectively. In addition, the top and bottom walls are assumed to be move in the x -direction with constant velocity, U_0 . Besides, slip conditions are imposed to these walls, while the other walls are considered to stationary. A uniform, horizontal magnetic field is considered with the following components:

$$B_y = 0, B_x = B_0 \quad (1)$$

Water is considered as a base fluid and copper is nanoparticles. The single phase nanofluid model is considered in which both the fluid phase and the nanoparticles are in thermal equilibrium state and move with the same local velocity. The effect of solid particle dispersion is taken into account, while the effects of Joule heating and viscous dissipation are neglected. The nanofluid thermophysical properties are assumed to be constants except for the nanofluid density which is determined using the Boussinesq approximation. Also, the thermophysical properties of the base fluid and nanoparticles are included in tab. 1.

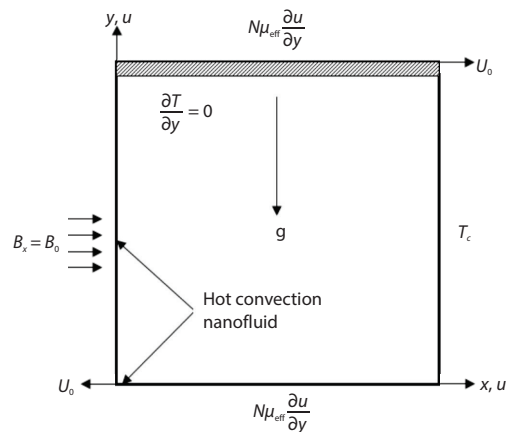


Figure 1. Physical model of the problem

Table 1. Thermophysical properties of water and copper nanoparticles material

Properties	ρ [kgm ⁻³]	C_p [Jkg ⁻¹ K ⁻¹]	k [Wm ⁻¹ K ⁻¹]	β [K ⁻¹]
Pure water	997.1	4179	0.613	$21 \cdot 10^{-5}$
Copper	8933	385	401	$1.67 \cdot 10^{-5}$

Mathematical analysis

Under the previous assumptions, the PDE governing the problem are expressed:
Subjected to the boundary conditions:

$$\frac{\partial u}{\partial x} + \frac{\partial v}{\partial y} = 0 \quad (2)$$

$$\rho_{nf,0} \left(u \frac{\partial u}{\partial x} + v \frac{\partial u}{\partial y} \right) = -\frac{\partial p}{\partial x} + \mu_{eff} \left[\frac{\partial^2 u}{\partial x^2} + \frac{\partial^2 u}{\partial y^2} \right] \quad (3)$$

$$\rho_{nf,0} \left(u \frac{\partial v}{\partial x} + v \frac{\partial v}{\partial y} \right) = -\frac{\partial p}{\partial y} + \mu_{eff} \left[\frac{\partial^2 v}{\partial x^2} + \frac{\partial^2 v}{\partial y^2} \right] +$$

$$+ \left[\phi \rho_{p,0} \beta_p + (1-\phi) \rho_{f,0} \beta_f \right] g (T - T_c) - \sigma_{nf} B_0^2 \sin^2 \left(\frac{\pi x}{H} \right) v \quad (4)$$

$$(\rho C)_{nf} \left(u \frac{\partial T}{\partial x} + v \frac{\partial T}{\partial y} \right) = \frac{\partial}{\partial x} \left[(k_{eff})_{stag} + k_d \right] \frac{\partial T}{\partial x} + \frac{\partial}{\partial y} \left[(k_{eff})_{stag} + k_d \right] \frac{\partial T}{\partial y} \quad (5)$$

Subjected to the following boundary conditions:

– on the left wall

$$u = v = 0, \quad -(k_{eff})_{stag} \frac{\partial T}{\partial x} = h(T - T') \quad (6a)$$

– on the right wall

$$u = v = 0, \quad T = T_c \quad (6b)$$

– on the bottom wall

$$u = \lambda_b U_0 + N \mu_{eff} \frac{\partial u}{\partial y}, \quad v = 0, \quad -\left[(k_{eff})_{stag} + k_d \right] \frac{\partial T}{\partial y} = h(T - T') \quad (6c)$$

– on the top wall

$$u = \lambda_t U_0 + N \mu_{eff} \frac{\partial u}{\partial y}, \quad v = 0, \quad \frac{\partial T}{\partial y} = 0 \quad (6d)$$

where (u, v) are the velocity components in the x - and y -directions, p – the pressure, T – the temperature, g – the gravity acceleration, H – the height of the cavity, μ – the dynamic viscosity, ρ – the density, β – the thermal expansion coefficient, σ – the electrical conductivity, k – the thermal conductivity, (ρC) – the heat capacitance, h – the heat transfer coefficient, N – the slip constant, λ – the constant moving parameter, T' – the temperature of the hot fluid, and the subscripts, t, b, and eff refer to top, bottom and effective, respectively.

The mathematical forms which determine the thermophysical properties of the nanofluid are given:

- the effective dynamic viscosity

$$\mu_{\text{eff}} = \frac{\mu_f}{(1-\phi)^{2.5}} \quad (7)$$

- the nanofluid density at the reference temperature

$$\rho_{\text{nf},0} = \phi\rho_{p,0} + (1-\phi)\rho_{f,0} \quad (8)$$

- the heat capacitance

$$(\rho C)_{\text{nf}} = \phi(\rho C)_p + (1-\phi)(\rho C)_f \quad (9)$$

- the effective thermal conductivity

$$k_{\text{eff}} = (k_{\text{eff}})_{\text{stag}} + k_d \quad (10)$$

where k_{eff} is the stagnant thermal conductivity and k_d – the enhancement in the thermal conductivity due to thermal dispersion, those are given, respectively:

$$\frac{(k_{\text{eff}})_{\text{stag}}}{k_f} = \frac{k_p + 2k_f - 2\phi(k_f - k_p)}{k_p + 2k_f + \phi(k_f - k_p)} \quad (11)$$

$$k_d = C\phi(\rho C)_{\text{nf}} d_p \sqrt{u^2 + v^2} \quad (12)$$

The electrical conductivity is given:

$$\frac{\sigma_{\text{nf}}}{\sigma_f} = 1 + \frac{3\phi\left(\frac{\sigma_p}{\sigma_f} - 1\right)}{\left(\frac{\sigma_p}{\sigma_f} + 2\right) - \left(\frac{\sigma_p}{\sigma_f} - 1\right)\phi} \quad (13)$$

where ϕ is the nanoparticle volume fraction, C – the constant, d_p – the nanoparticle diameter, and the subscripts f, p, and 0 refer to the base fluid, nanoparticle and reference state, respectively.

The following dimensionless variables are introduced:

$$X = \frac{x}{H}, \quad Y = \frac{y}{H}, \quad U = \frac{u}{U_0}, \quad V = \frac{v}{U_0}, \quad P = \frac{p}{\rho_{\text{nf},0}U_0^2}, \quad \theta = \frac{T - T_c}{T' - T_c} \quad (14)$$

Substituting eq. (14) into eqs. (2)-(5), the following dimensionless system is obtained:

$$\frac{\partial U}{\partial X} + \frac{\partial V}{\partial Y} = 0 \quad (15)$$

$$U \frac{\partial U}{\partial X} + V \frac{\partial U}{\partial Y} = -\frac{\partial P}{\partial X} + \frac{\mu_{\text{eff}}}{\rho_{\text{nf},0}} \frac{\rho_{f,0}}{\mu_f} \frac{1}{\text{Re}} \left[\frac{\partial^2 U}{\partial X^2} + \frac{\partial^2 U}{\partial Y^2} \right] \quad (16)$$

$$U \frac{\partial V}{\partial X} + V \frac{\partial V}{\partial Y} = -\frac{\partial P}{\partial Y} + \frac{\mu_{\text{eff}}}{\rho_{\text{nf},0}} \frac{\rho_{\text{f},0}}{\mu_{\text{f}}} \frac{1}{\text{Re}} \left[\frac{\partial^2 V}{\partial X^2} + \frac{\partial^2 V}{\partial Y^2} \right] +$$

$$+ \frac{\text{Gr}}{\text{Re}^2} \left[\frac{1}{1 + \frac{(1-\phi) \rho_{\text{f},0}}{\phi \rho_{\text{p},0}}} \frac{\beta_{\text{p}}}{\beta_{\text{f}}} + \frac{1}{1 + \frac{\phi \rho_{\text{p},0}}{(1-\phi) \rho_{\text{f},0}}} \right] \theta - \frac{\sigma_{\text{nf}}}{\sigma_{\text{f}}} \frac{\rho_{\text{f},0}}{\rho_{\text{nf},0}} \frac{\text{Ha}^2}{\text{Re}} \sin^2(\pi X) V \quad (17)$$

$$U \frac{\partial \theta}{\partial X} + V \frac{\partial \theta}{\partial Y} = \frac{1}{\text{RePr}} \left[\frac{\partial}{\partial X} (\chi) \frac{\partial \theta}{\partial X} + \frac{\partial}{\partial Y} (\chi) \frac{\partial \theta}{\partial Y} \right] \quad (18)$$

where

$$\chi = \frac{\frac{(k_{\text{eff}})_{\text{stag}}}{k_{\text{f}}}}{(1-\phi) + \phi \frac{(\rho C)_{\text{p}}}{(\rho C)_{\text{f}}}} + \text{RePr} C \phi \frac{d_{\text{p}}}{H} \sqrt{U^2 + V^2}$$

The dimensionless boundary conditions are:

– on the left wall

$$U = V = 0, \quad \frac{(k_{\text{eff}})_{\text{stag}}}{k_{\text{f}}} \frac{\partial \theta}{\partial X} = -\text{Bi}(1-\theta) \quad (19a)$$

– on the right wall

$$U = V = 0, \quad \theta = 0 \quad (19b)$$

– on the bottom wall

$$U = \lambda_{\text{b}} + S_{\text{b}} \frac{\mu_{\text{eff}}}{\mu_{\text{f}}} \frac{\partial U}{\partial Y}, \quad V = 0, \quad \left[\frac{(k_{\text{eff}})_{\text{stag}}}{k_{\text{f}}} + k_{\text{d}}^* \right] \frac{\partial \theta}{\partial Y} = -\text{Bi}(1-\theta) \quad (19c)$$

– on the top wall

$$U = \lambda_{\text{t}} + S_{\text{t}} \frac{\mu_{\text{eff}}}{\mu_{\text{f}}} \frac{\partial U}{\partial Y}, \quad V = 0, \quad \frac{\partial \theta}{\partial y} = 0 \quad (19d)$$

where

$$k_{\text{d}}^* = C \text{Re} \text{Pr} \phi U \frac{d_{\text{p}}}{H} \left[(1-\phi) + \phi \frac{(\rho C)_{\text{p}}}{(\rho C)_{\text{f}}} \right], \quad \text{Gr} = \frac{g \beta_{\text{f}} H^3 (T' - T_{\text{c}})}{\nu_{\text{f}}^2} \text{ is the Grashof number}$$

$$\text{Re} = \frac{U_0 H}{\nu_{\text{f}}} \text{ is the Reynolds number, } \text{Pr} = \frac{\nu_{\text{f}} (\rho C)_{\text{f}}}{k_{\text{f}}} \text{ is the Prandtl number}$$

$$\text{Ha} = B_0 H \sqrt{\frac{\sigma_{\text{f}}}{\mu_{\text{f}}}} \text{ is the Hartman number, } S_{\text{b}} = S_{\text{t}} = \frac{N \mu_{\text{f}}}{H} \text{ is the dimensionales parameter}$$

$$\text{Bi} = \frac{hH}{k_{\text{f}}} \text{ is the Biot number}$$

The local Nusselt number at the left wall is defined:

$$\text{Nu} = \frac{q_w H}{k_f (T' - T_c)} = - \frac{H (k_{\text{eff}})_{\text{stag}}}{k_f (T' - T_c)} \left. \frac{\partial T}{\partial X} \right|_{X=0} \quad (20)$$

Using the dimensionless variable eq. (12), then eq. (20) is converted:

$$\text{Nu} = - \frac{(k_{\text{eff}})_{\text{stag}}}{k_f} \left. \frac{\partial \theta}{\partial X} \right|_{X=0} \quad (21)$$

The average Nusselt number is defined:

$$\text{Nu}_{\text{av}} = \int_0^1 \text{Nu} dY \quad (22)$$

Further, the stream function is defined in usual way:

$$\frac{\partial^2 \psi}{\partial X^2} + \frac{\partial^2 \psi}{\partial Y^2} = \frac{\partial U}{\partial Y} - \frac{\partial V}{\partial X} \quad (23)$$

The present simulation methodology

The governing eqs. (15)-(18) with the boundary conditions (19) were solved, numerically, using the finite volume method as explained in Ahmed [28]. The convective term was treated using the first order upwind scheme, while the second order difference scheme was used for the diffusive term. The Rhie and Chow's momentum interpolation was applied to obtain the cell face velocity, U_e :

$$U_e = f_e^* U_E + (1 - f_e^*) U_P - \frac{\alpha_u \Delta Y (P_E - P_p)}{(a_p^u)_e} + f_e^* \frac{\alpha_u \Delta Y (P_e - P_w)_E}{(a_p^u)_E} + (1 - f_e^*) \frac{\alpha_u \Delta Y (P_e - P_w)_p}{(a_p^u)_p} \quad (24)$$

where

$$f_e^* = \frac{\Delta X_p}{2 \delta x_e}, \quad \frac{1}{(a_p^u)_e} = f_e^* \frac{1}{(a_p^u)_E} + (1 - f_e^*) \frac{1}{(a_p^u)_p}$$

The SIMPLE algorithm was applied to correct the guessed pressure and velocity fields. The resultant algebraic system was solved using alternating direct implicit procedure. The convergence criteria were set 10^{-6} and the grid size 81×81 was found to be suitable for the computations. The present results are compared, in special cases of the present study, with previously published results. Figure 2(a) shows an excellent agreement is observed between the current results and those obtained by Iwatsu *et al.* [29] and Khanafer and Chamkha [30]. Also, another comparison is performed in case of nanofluid with Rashad *et al.* [14] and presented on fig. 2(b). As it can be observed, the streamlines and isotherms are almost the same and these confirm that the current results are very accurate.

Results and discussion

Here, the numerical results are discussed. The computations are carried out for wide ranges of the governing parameter. In this study, the Biot number varies from 0.1-10, the slip

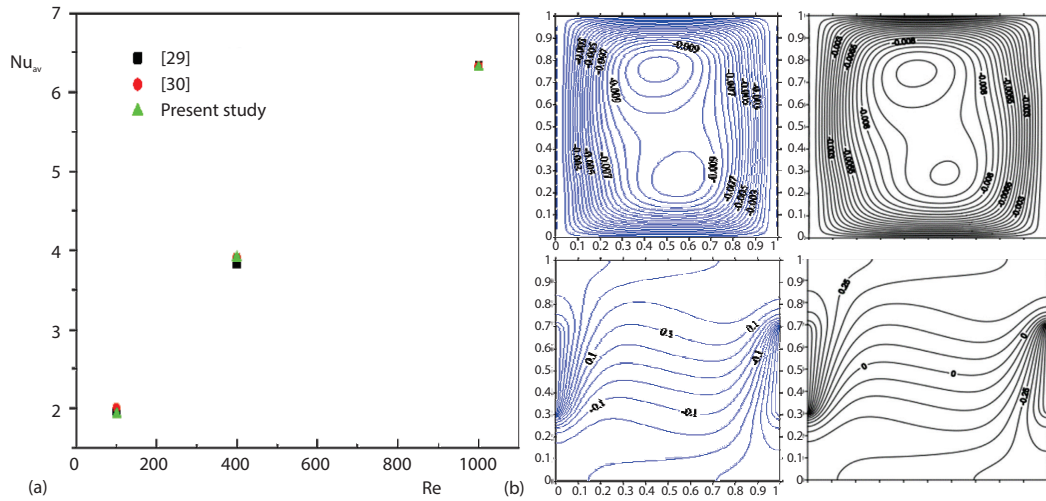


Figure 2. (a) Validation test at $Pr = 0.71$, $Gr = 100$, $S_b = S_t = Bi = Ha = \phi = 0$, present results Rashad *et al.* [14] and (b) comparisons of the present results with those of Rashad *et al.* [14] in case of nanofluid at $B = 0.4$, $D = 0.5$, $Ri = 1$, $Ha = 10$, $\phi = 5\%$, $\lambda_t = \lambda_b = -1$, $S_b = S_t = 1$

parameters S_b and S_t vary from 0-10, the nanoparticle volume fraction ϕ varies from 0-10% and the Hartmann number varies from 0-10. Any of the following figures were produced at referenced values of the governing parameters. These values are $Bi = 1$, $Re = 100$, $Pr = 6.2$, $Ge = 10^4$, $Ha = 10$, $\phi = 0.06$, $\lambda_t = -\lambda_b = 1$, $S_b = S_t = 1$. Figures 3 shows the contours of the streamlines and isotherms for the variations of Biot number. The results revealed that for the low values of Biot number ($Bi = 0.1$), there are three vortices formulated inside the enclosure. Two of them near the moving walls and stretch horizontally due to the walls movements. Further, the streamlines gathering near the moving walls indicating a big shear stress resulting from the slip-condition. A good thermal cavity is obtained with parallel paths and low maximum temperatures at the low values of Biot number. Increase the Biot number causes a mingle of the mentioned vortices to form a large cell occupied the entire area of the enclosure. The fluid-flow, also, increases,

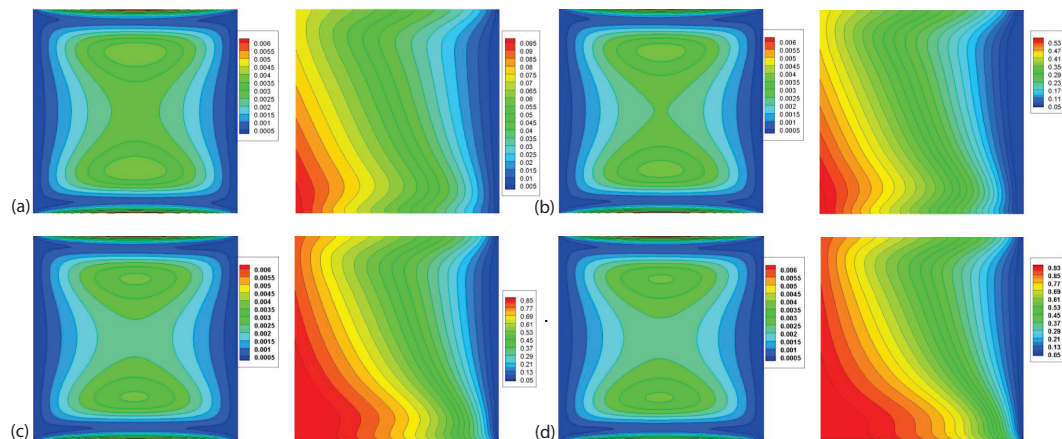


Figure 3. Contours of streamlines and isotherms for different values of Bi at $Re = 100$, $Pr = 6.2$, $Gr = 10^4$, $Ha = 10$, $\phi = 0.1$, $\lambda_t = -\lambda_b = 1$, $S_b = S_t = 0.1$; (a) $Bi = 0.1$, (b) $Bi = 1$, (c) $Bi = 5$, and (d) $Bi = 10$

gradually, pointing a good mixed convection as Biot number increases. As anticipated, the maximum temperature is enhanced by increasing the Biot number and crowded near the cold wall indicating to an extra heat transfer. Moreover, the nanofluid-flow tapers near the walls where the convective boundary conditions occurred and the temperature distributions move away to the right-hand side of the cavity. In addition, fig. 4 shows that the velocity components are reduced as Biot number increases, while, the heat transfer rate grow, slightly, by increasing the Biot number. However, the high values of Biot number ($Bi = 10$) cause that the local Nusselt number tends to decrease.

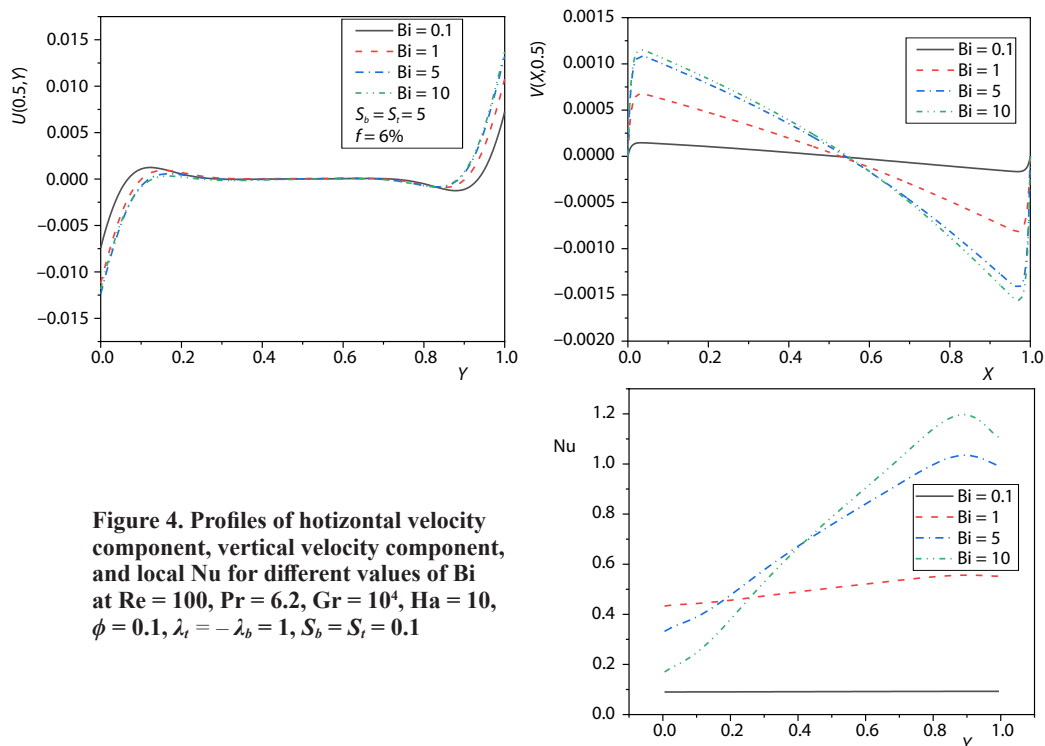


Figure 4. Profiles of horizontal velocity component, vertical velocity component, and local Nu for different values of Bi at $Re = 100$, $Pr = 6.2$, $Gr = 10^4$, $Ha = 10$, $\phi = 0.1$, $\lambda_t = -\lambda_b = 1$, $S_b = S_t = 0.1$

Effects of slip-parameters (S_b and S_t) on the streamlines and isotherms are examined using fig. 5. It is found that in absence of slip-condition ($S_t = S_b = 0$), effects of the shear stress resulting from the lid-driven cavity are high and the fluid-flow is represented by three eddies. Two of them are in clockwise direction and the other is in anticlockwise direction. The isotherms leave the hot walls heading to the cold wall indicating a very heated region near this wall (right wall). Besides, the fluid motion and temperature distributions are very sensitive to the increase in slip-parameters. A low variation of S_b and S_t ($S_b = S_t = 1$) (gives high effects on the streamlines and isotherms. The referred eddies overlap each to form one vortex inside the enclosure. A low maximum temperature is obtained with uniform distributions is obtained by increasing S_b and S_t . More increases in the slip parameters leads to decrease the mixed convection and, consequently, the maximum temperature. The horizontal velocity component is reduced, sharply, as S_b and S_t increase, while the vertical velocity component behaviour in case of S_b and $S_t > 0$ is, approximately, opposite to its behavior in the case of $S_b = S_t = 0$. The heat transfer rate increases by 8.45%, 9.54%, and 9.58% as S_b and S_t increases from 1-5, respectively compared with $S_b = S_t = 0$. The average Nusselt number is reduced as slip parameters increases,

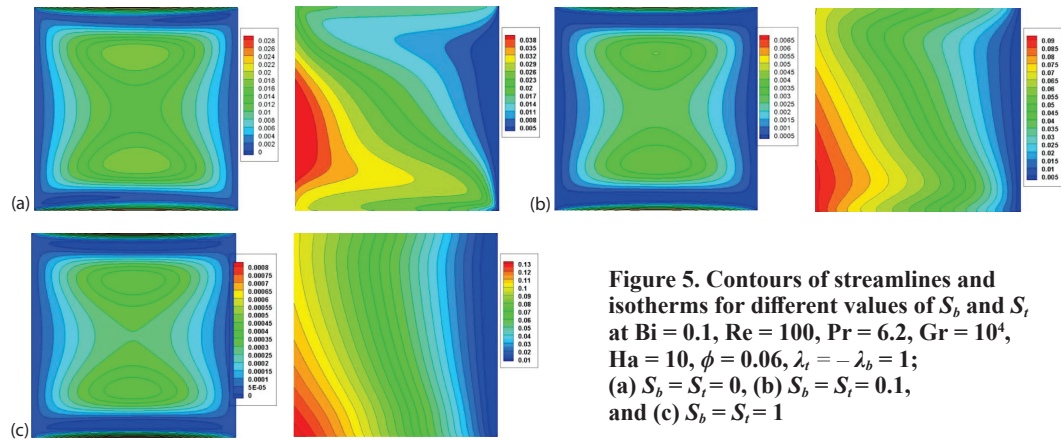


Figure 5. Contours of streamlines and isotherms for different values of S_b and S_t at $Bi = 0.1$, $Re = 100$, $Pr = 6.2$, $Gr = 10^4$, $Ha = 10$, $\phi = 0.06$, $\lambda_t = -\lambda_b = 1$; (a) $S_b = S_t = 0$, (b) $S_b = S_t = 0.1$, and (c) $S_b = S_t = 1$

while it increases by increasing the Biot number. On contrary, extra increase in the Biot number makes the average Nusselt number tends to decrease. The aforementioned profiles of the velocity components, local and average Nusselt numbers under effects of variations of the Biot number are presented in fig. 6.

In fig. 7, effects of the nanoparticle volume fraction, ϕ , on the streamlines and isotherms contours are determined. It is observed that a single vortex is performed in the cavity

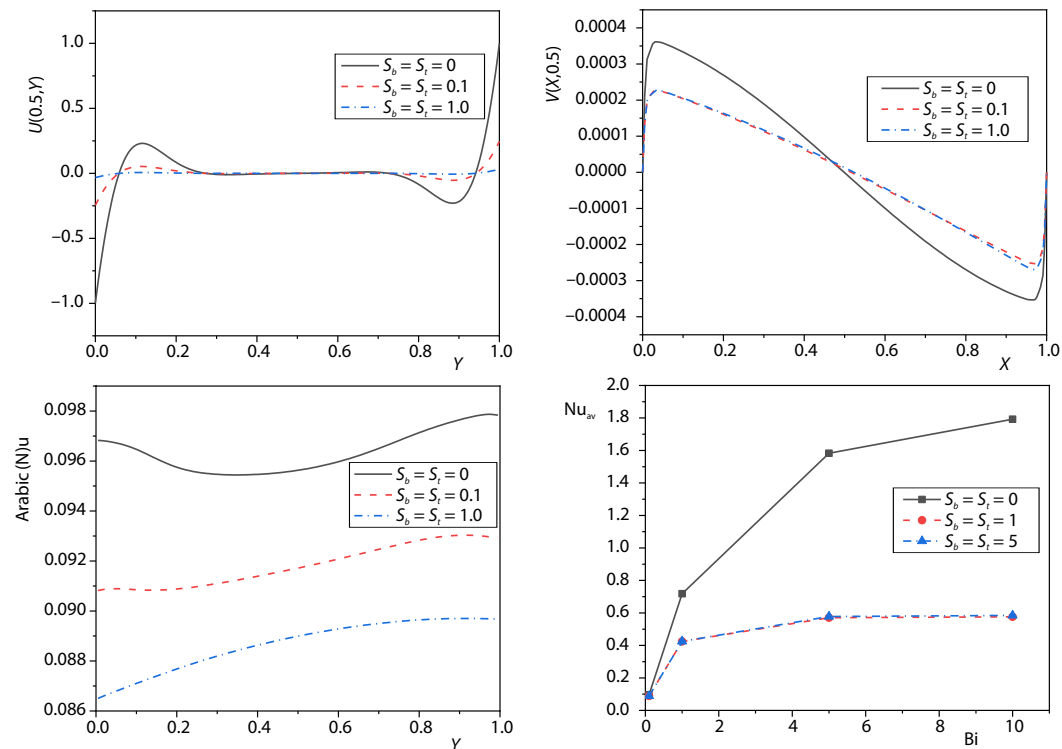


Figure 6. Profiles of horizontal velocity component, vertical velocity component, local and average Nu for different values of S_b and S_t at $Bi = 0.1$, $Re = 100$, $Pr = 6.2$, $Gr = 10^4$, $Ha = 10$, $\phi = 0.06$, $\lambda_t = -\lambda_b = 1$

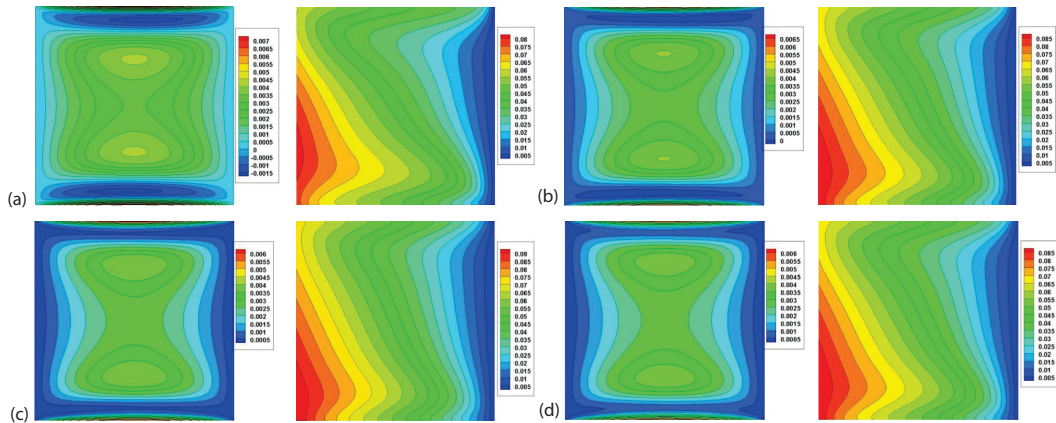


Figure 7. Contours of streamlines and isotherms for different values of ϕ at $Bi = 0.1$, $Re = 100$, $Pr = 6.2$, $Gr = 10^4$, $Ha = 10$, $\lambda_t = -\lambda_b = 1$, $S_b = S_t = 0.1$; (a) $\phi = 0.01$, (b) $\phi = 0.05$, (c) $\phi = 0.08$, and (d) $\phi = 0.1$

with strong friction forces near the moving walls at $\phi = 1\%$. Besides, good distributions for the isotherms are noted with gathering of lines near the right wall, particularly, beside the right corner. Increase the amount of nanoparticles in the base fluid (ϕ increases) acts as a retarding force for the nanofluid motion and decreases the shear-friction near the horizontal walls as well. The isotherms bulk near the top right wall tends to decrease as ϕ increases till vanishes at $\phi = 10\%$. Also, it can be seen that enlargement of the vortex is reduced accompanied by the appearance of an empty area in the cavity core and this area increases as ϕ increases. In fig. 8, profiles of

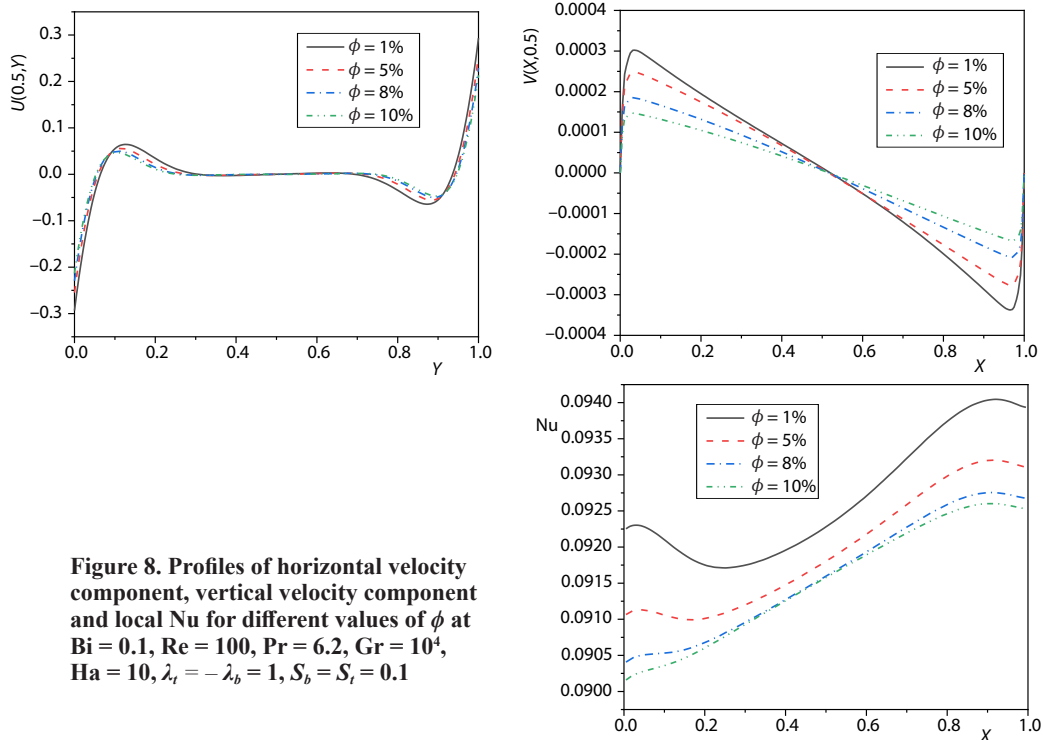


Figure 8. Profiles of horizontal velocity component, vertical velocity component and local Nu for different values of ϕ at $Bi = 0.1$, $Re = 100$, $Pr = 6.2$, $Gr = 10^4$, $Ha = 10$, $\lambda_t = -\lambda_b = 1$, $S_b = S_t = 0.1$

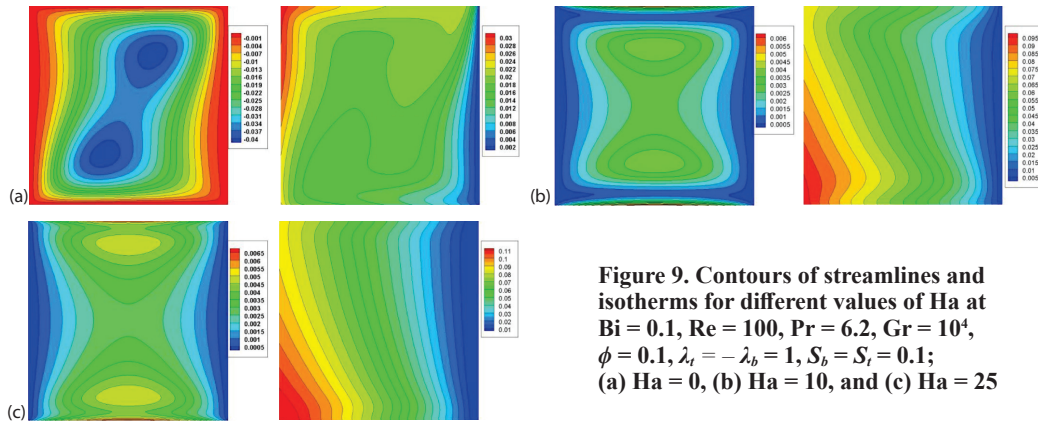


Figure 9. Contours of streamlines and isotherms for different values of Ha at Bi = 0.1, Re = 100, Pr = 6.2, Gr = 10⁴, $\phi = 0.1, \lambda_t = -\lambda_b = 1, S_b = S_t = 0.1$; (a) Ha = 0, (b) Ha = 10, and (c) Ha = 25

the velocity components and local Nusselt number under effects of the nanoparticle volume fraction ϕ is presented. It is noted that an increase in nanoparticle volume fraction ϕ causes an enhancement in profiles of $U(0.5, Y)$ in the lower part of the enclosure while in the upper part, the horizontal velocity component is reduced. The same is valid for the vertical velocity but in the right and left parts. The local Nusselt shrinks by increasing the nanoparticle volume fraction and this is due to that the effects of slip condition that is dominance than the effect of ϕ .

Effects of the variations of the Hartmann number on the streamlines and isotherms contours are found in fig. 9. It is observed that at Ha = 0, the drag caused by the moving lids

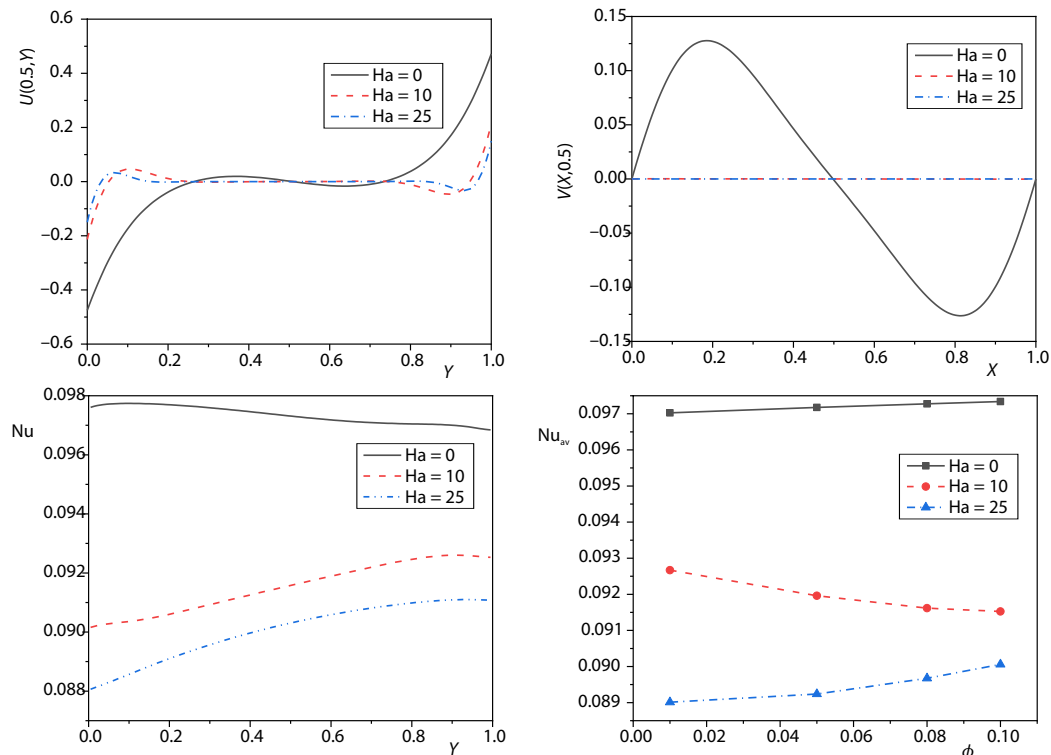


Figure 10. Profiles of horizontal velocity, vertical velocity components, local and average Nu for different values of Ha at Bi = 0.1, Re = 100, Pr = 6.2, Gr = 10⁴, $\phi = 0.1, \lambda_t = -\lambda_b = 1, S_b = S_t = 0.1$

is small comparing with the buoyancy force. Also, the shear-friction vanishes and the heat transfer takes its maximum in this case. As Hartmann number increases, the mixed convection mode starts to dominate. Both the effects of slip-conditions and lid-driven forces on the horizontal walls increase as Hartmann number increases. Also, the maximum temperature is enhanced by increasing Hartmann number. More increase in Hartmann number causes that the wavy distributions of the Lorentz force is enhanced and thus decreases the fluid activity. While on contrary, the maximum temperature inside the enclosure increases and thus the rate of heat transfer decreases, sharply, as Hartmann number increases from 0-10 and it increases gradually, as Ha increases from 10-25. Figure 10 shows the profiles of the velocity components $U(0.5, Y)$ and $V(X, 0.5)$ at the enclosure mid-section and the local Nusselt number at the left wall as well as the average Nusselt number under the effect of variations of Hartmann number. It is noted that there are a sharply reduction in the profiles of $U(0.5, Y)$, $V(X, 0.5)$, Nu and Nu_{av} as Hartmann number varies from 0 to 10, while as Hartmann number increases from 10-25 causes in gradually decrease in the profiles of $U(0.5, Y)$, $V(X, 0.5)$, Nu and Nu_{av} . In addition, at $Ha = 0$ and $Ha = 25$, the average Nusselt number increases as nanoparticle volume fraction increases, while the opposite behavior is noted at $Ha = 10$.

Conclusions

The steady 2-D flow of nanofluids in a double lid-driven cavity in the presence of a wavy magnetic field was investigated in the current article. Effects of slip conditions on the moving walls as well as effects of convective boundary conditions on two adjacent walls of the cavity were taken into account. The governing equations were solved numerically using the finite volume method and comparisons with previously published results was conducted and found in an excellent agreement. From this study, the following conclusions can be reported as follows.

- The increase in the slip parameter causes a clear reduction in the horizontal velocity component, local and average Nusselt number, while the behavior of the vertical velocity component in case of absence of slip condition is completely inverse to its behavior in case of presence of slip condition.
- The rate of heat transfer increases as the Biot number increases; while more increase in this number reduces the local Nusselt number.
- The increase in the Hartman number increases the shear friction near the moving walls; however, a slightly reduction in the velocity components, local and average Nusselt number is obtained as the Hartman number increases.
- The rate of heat transfer enhancement is obtained by increasing the nanoparticle volume fraction, only in case of higher values of the Hartman number.

Acknowledgment

The authors extend their appreciation to the Deanship of Scientific Research at King Khalid University, Abha, Saudi Arabia, for funding this work through the Research Group Project under Grant Number (RGP.1/19/42).

References

- [1] Chol, S., Eastman, J. A., Enhancing Thermal Conductivity of Fluids with Nanoparticles, *ASME-Publications-Fed*, 231 (1995), Jan., pp. 99-106
- [2] Eastman, J. A., *et al.*, Anomalous Increased Effective Thermal Conductivities of Ethylene Glycol-Based Nanofluids Containing Copper Nanoparticles, *Applied Physics Letters*, 78 (2001), 6, pp. 718-720
- [3] Mansour, M. A., *et al.*, Numerical Simulation of Mixed Convection Flows in a Square Lid-Driven Cavity Partially Heated from below Using Nanofluid, *International Communications in Heat and Mass Transfer*, 10 (2010), 10, pp. 1504-1512

- [4] Mansour, M., Ahmed, S. E., Mixed Convection in Double Lid-Driven Enclosures Filled With Al_2O_3 -Water Nanofluid, *Journal of Thermophysics and Heat Transfer*, 27 (2013), 4, pp. 707-718
- [5] Hayat, T., et al., Comparative Study of Silver and Copper Wnanofluids with Mixed Convection and Non-Linear Thermal Radiation, *International Journal of Heat and Mass Transfer*, 102 (2016), Nov., pp. 723-732
- [6] Chen, B.-S., Liu, C.-C., Entropy Generation in Mixed Convection Magnetohydrodynamic Nanofluid-Flow in Vertical Channel, *International Journal of Heat and Mass Transfer*, 91 (2015), Dec., pp. 1026-1033
- [7] Selimefendigil, F., Oztop, H. F., Analysis of MHD Mixed Convection in a Flexible Walled and Nanofluids Filled Lid-Driven Cavity with Volumetric Heat Generation, *International Journal of Mechanical Sciences*, 118 (2016), Nov., pp. 113-124
- [8] Rashidi, M. M., et al., Numerical Investigation of Magnetic Field Effect on Mixed Convection Heat Transfer of Nanofluid in a Channel with Sinusoidal Walls, *Journal of Magnetism and Magnetic Materials*, 401 (2016), Mar., pp. 159-168
- [9] Hsiao, K.-L., Stagnation Electrical MHD Nanofluid Mixed Convection with Slip Boundary on a Stretching Sheet, *Applied Thermal Engineering*, 98 (2016), Apr., pp. 850-861
- [10] Sankar, M., et al., Natural-Convection in a Non-Uniformly Heated Vertical Annular Cavity, *Defect and Diffusion Forum*, 377 (2017), Sept., pp. 189-199
- [11] Mahajan, A., et al., Penetrative Internally Heated Convection in Magnetic Fluids, *Defect and Diffusion Forum*, 387 (2018), Sept., pp. 373-384
- [12] Das, S., et al., Influence of Wall Conductivities on a Fully Developed Mixed-Convection Magnetohydrodynamic Nanofluid-Flow in a Vertical Channel, *Journal of Engineering Physics and Thermophysics*, 91 (2018), 3, pp. 784-796
- [13] Ismael, M. A., et al., Mixed Convection in a Nanofluid Filled-Cavity with Partial Slip Subjected to Constant Heat Flux and Inclined Magnetic Field, *Journal of Magnetism and Magnetic Materials*, 416 (2016.), Suppl. C, pp. S25-S36
- [14] Rashad, A. M., et al., The MHD Mixed Convection of Localized Heat Source/Sink in a Nanofluid-Filled Lid-Driven Square Cavity with Partial Slip, *Journal of the Taiwan Institute of Chemical Engineers*, 68 (2016.), Suppl. C, pp. S173-S186
- [15] Hayat, T., et al., Investigation of Hall Current and Slip Conditions on Peristaltic Transport of Cu-Water Nanofluid in a Rotating Medium, *International Journal of Thermal Sciences*, 112 (2017), Feb., pp. 129-141
- [16] Alsabery, A., et al., Transient Free Convective Heat Transfer in Nanoliquid-Saturated Porous Csquare Cavity with a Concentric Solid Insert and Sinusoidal Boundary Condition, *Superlattices and Microstructures*, 100 (2016), Dec., pp. 1006-1028
- [17] Djoko, J., Koko, J., Numerical Methods for the Stokes and Navier-Stokes Equations Driven by Threshold Slip Boundary Conditions, *Computer Methods in Applied Mechanics and Engineering*, 305 (2016), June, pp. 936-958
- [18] Abbas, Z., Sheikh, M., Numerical Study of Homogeneous-Heterogeneous Reactions on Stagnation Point Flow of Ferrofluid with Non-Linear Slip Condition, *Chinese Journal of Chemical Engineering*, 25 (2017), 1, pp. 11-17
- [19] Akbar, N. S., Khan, Z. H., Effect of Variable Thermal Conductivity and Thermal Radiation with CNTS Suspended Nanofluid over a Stretching Sheet with Convective Slip Boundary Conditions: Numerical study, *Journal of Molecular Liquids*, 222 (2016), Oct., pp. 279-286
- [20] Mansour, M., et al., Fluctuating Thermal and Mass Diffusion on Unsteady MHD Convection of a Micro Polar Fluid through a Porous Medium Past a Vertical Plate in Slip-Flow Regime, *International Journal of Applied Mathematics and Mechanics*, 3 (2007), pp. 99-117
- [21] Murthy, P., et al., Magnetic Effect on Thermally Stratified Nanofluid Saturated Non-Darcy Porous Medium under Convective Boundary Condition, *International Communications in Heat and Mass Transfer*, 47 (2013), Oct., pp. 41-48
- [22] Aziz, A., A Similarity Solution for Laminar Thermal Boundary-Layer over a Flat Plate with a Convective Surface Boundary Condition, *Communications in Non-Linear Science and Numerical Simulation*, 14 (2009), 4, pp. 1064-1068
- [23] Makinde, O. D., Aziz, A., Boundary-Layer Flow of a Nanofluid Past a Stretching Sheet with a Convective Boundary Condition, *International Journal of Thermal Sciences*, 50 (2011), 7, pp. 1326-1332
- [24] Ishak, A., Similarity Solutions for Flow and Heat Transfer over a Permeable Surface with Convective Boundary Condition, *Applied Mathematics and Computation*, 217 (2010), 2, pp. 837-842

- [25] Bachok, N., *et al.*, Flow and Heat Transfer at a General 3-D Stagnation Point in a Nanofluid, *Physica B: Condensed Matter*, 405 (2010), 24, pp. 4914-4918
- [26] Ahmad, S., Pop, I., Mixed Convection Boundary-Layer Flow from a Vertical Flat Plate Embedded in a Porous Medium Filled with Nanofluids, *International Communications in Heat and Mass Transfer*, 37 (2010), 8, pp. 987-991
- [27] Bataller, R. C., Similarity Solutions for Flow and Heat Transfer of a Quiescent Fluid over a Non-Linearly Stretching Surface, *Journal of Materials Processing Technology*, 203 (2008), 1-3, pp. 176-183
- [28] Ahmed, S. E., Mixed Convection in Thermally Anisotropic Non-Darcy Porous Medium in Double Lid-Driven Cavity Using Bejan's Heatlines, *Alexandria Engineering Journal*, 55 (2016), 1, pp. 299-309
- [29] Iwatsu, R., *et al.*, Mixed Convection in a Driven Cavity with a Stable Vertical Temperature Gradient, *International Journal of Heat and Mass Transfer*, 36 (1993), 6, pp. 1601-1608
- [30] Khanafer, K. M., Chamkha, A. J., Mixed Convection Flow in a Lid-Driven Enclosure Filled with a Fluid-Saturated Porous Medium, *Int. J. Heat Mass Transfer*, 42 (1999), 13, pp. 2465-2481